Polyacrylonitrile-Based Electrospun Carbon Paper for Electrode Applications

Ying Yang,[1,2] Fritz Simeon,[1] T. Alan Hatton,[1] Gregory C. Rutledge[1]

[1]*Department of Chemical Engineering, Massachusetts Institute of Technology, Cambridge, Massachusetts 02139*
[2]*Department of Electrical Engineering, Tsinghua University, Beijing 100084, China*

Received 13 July 2011; accepted 2 August 2011
DOI 10.1002/app.35485
Published online 27 November 2011 in Wiley Online Library (wileyonlinelibrary.com).

ABSTRACT: Polyacrylonitrile (PAN)-based carbon paper with fiber diameters of 200–300 nm was developed through hot-pressing, pre-oxidation, and carbonization of electrospun fiber mats. Changes in morphology, crystallinity, and surface chemistry of the hot-pressed carbon paper were investigated. More junctions between fibers were formed with increasing hot-press time, which is attributed to melting and bonding of fibers. The bulk density increased to 0.5–0.6 g/cm^3, which could help to improve the volume energy density for electrode applications. The conductivity of the carbon paper was found to be about 40 S/cm when the surface area was $\sim$ 2 m^2/g, and depends not only on the conductivity of the individual nanofibers but also on the contacts between the nanofibers. The performance of the electrospun carbon paper as an electrode for electrochemical reactions involving ferrocene molecules was affected by the preparation protocol: the higher surface area of the electrodes formed with shorter hot-press times provided a higher current generated per unit mass than that obtained with electrodes prepared using longer hot-press time, but electrodes prepared with longer hot-press times exhibited higher electrical conductivity and faster electron transfer kinetics. © 2011 Wiley Periodicals, Inc. J Appl Polym Sci 124: 3861–3870, 2012

Key words: electrospinning; PAN; hot-press; carbon fiber; electrode

INTRODUCTION

Carbon fibers are used widely as electrodes for fuel cells,[1] supercapacitors,[2] redox flow batteries,[3] and other electrochemical processes, since they are typically porous, electrically and ionically conducting, electrochemically inert, and have high surface areas. Electrospinning technology has emerged in recent years as a simple and effective approach to produce high surface area membranes from either polymer solutions or melts.[4,5] Almost any polymer that is sufficiently soluble and of high molecular weight can be electrospun, provided that the resulting solution or melt has the necessary electrical and viscoelastic properties.[6,7] Recently, electrospun polyacrylonitrile (PAN)-based or pitch-based carbon fibers with diameters of a few hundreds of nanometers have been reported.[7–16]

Most of the research work is focused on improving the energy density of the electrode, including improving the surface area and pore distribution of the electrode,[12–16] since these heterogeneous electron transfer processes occur only at the interface between the solid electrode and the redox chemistry-containing phases. Another challenge to which more attention should be paid is the enhancement of the power density of the electrode, which is related more to the conductivity of the carbon fibers in real applications, especially in redox flow battery systems. The conductivity of electrospun carbon fiber is usually below 20 S/cm.[12–16] It is noteworthy that the reported carbon nanofibers were carbonized directly from the electrospun nanofiber mats, which are usually fluffy or with poor bonding between fibers. However, for electrode applications, there are two points that have to be considered: (1) the electrical conductivity of a carbon paper depends not only on the conductivity of the individual fibers but also on the network of interconnections between multiple fibers and (2) the mechanical properties (e.g., Young's modulus, toughness, etc.) of the carbon fibers from as-spun polymeric fibers are relatively poor, rendering the resulting electrospun carbon paper (ECP) unsuitable for use directly as an electrode. Zhou et al. reported that the electrical conductivity of a nanofiber bundle is determined not only by the conductivity of individual nanofibers in the bundle but also by the adhesive contacts and/or entanglements among the nanofibers.[9] Hot-press treatment has been proposed as one method to improve the adhesion between fibers in electrospun mats. Yuan and coworkers reported that the mechanical

Additional Supporting Information may be found in the online version of this article

Correspondence to: Y. Yang (yingyang@tsinghua.edu.cn) or G. C. Rutledge (rutledge@mit.edu).

properties of electrospun polyvinylidene fluoride (PVDF) membranes were remarkably enhanced by hot-press treatment, whereas the porosity and the liquid absorption capacity decreased.[17,18] A hot-press post-treatment could be a feasible method to produce electrospun membranes with better electrical and mechanical connections between fibers, and is not limited to PVDF.

In this study, a hot-press treatment was used to modify an electrospun PAN precursor. The effect of hot-press time on the ultimate electrical and mechanical properties of electrospun PAN-based carbon paper was investigated systematically. X-ray diffractometry (XRD), Raman spectroscopy, X-ray photoelectron spectroscopy (XPS), and Fourier-transform infrared spectroscopy (FTIR) (Supporting Information) were used to reveal the microstructure and composition of the carbon fibers. Impedance spectroscopy was used to measure the conductivity of the carbon fiber paper. The electrochemical reaction of ferrocene molecules was used to characterize the carbon fiber paper with the aim of evaluating its electrode performance.

EXPERIMENTAL

Materials

PAN (M_w 150 kDa) was purchased from Polysciences Inc. (Warrington, PA) and used as received. *N*,*N*-Dimethyl formamide (DMF) was purchased from Sigma–Aldrich Chemical Co. (St. Louis, MO) and used as received. Ten weight percent of PAN/DMF solution was prepared by directly adding the PAN polymer to DMF with vigorous stirring for at least 3–4 h at 80°C.

Electrospinning

A parallel-plate electrospinning apparatus was used in this study, as described by Shin et al.[19] A syringe pump (Harvard Apparatus PHD 2000) was used to deliver polymer solution via a Teflon feed line to a capillary nozzle. Voltages up to 30 kV, generated by a power supply (Gamma High Voltage Research ES-30P), were applied between the upper plate and the grounded plate to provide the driving force for electrospinning. Typically, the electrical potential was 30 kV, the solution flow rate was 0.025 mL/min, and the distance between the capillary nozzle and the collector was 35 cm to ensure the formation of a stable jet. The fibers were collected on a grounded, flat, non-stick aluminum foil sheet.

Hot-pressing, pre-oxidation, and carbonization

Prior to pre-oxidation, the peeled electrospun PAN membrane was folded and placed in a hot-press (Carver model 3912) set at zero pressure until the temperature of the plates reached 200°C, typically about 30 min. Then, 400 kPa pressure was applied between the plates for periods of 5, 25, 40, and 60 min. Next, the pressure was released completely and the sample was allowed to cool down to room temperature, typically about 60 min. The pre-oxidation step was carried out in a box furnace (Lindberg, 1100°C Moldatherm® Box Furnace) by heating the hot-pressed PAN membrane from room temperature to 270°C with the heating rate set at 5°C/min in air, followed by holding the temperature at 270°C for 90 min to complete the stabilization. The stabilized membrane was then carbonized at 1000°C in a high purity nitrogen environment in a tube furnace (Lindberg/Blue M 1100°C Tube Furnace) with a heating rate of 3°C/min. All of the carbonized PAN membranes were held at 1000°C for 1 h to allow the carbonization to go to completion. During the heat-treatment, two 5-mm thick molybdenum (Mo) plates were used to make a Mo-PAN-Mo sandwich fixed by Mo wire in order to keep the mat flat. No additional pressure was applied to the sample during pre-oxidation or carbonization.

Characterization

Morphological characterization was performed by scanning electron microscopy (SEM) (JEOL-6060SEM, JEOL Ltd., Japan). For XRD studies, a PANalytical X'Pert Pro Multipurpose Diffractometer was operated at 45 kV and 40 mA with Cu Kα radiation (wavelength 1.540598 Å) at a scanning speed of 3°/min. A Horiba Jobin Yvon Labram HR800 spectrometer was used for recording the Raman spectra with excitation wavelength 633.0 nm at 3 mW of laser power. XPS (Kratos Analytical, Manchester) measurements were recorded with a Kratos Axis Ultra instrument equipped with a monochromatic Al Kα source operated at 150 W. The analyzer angle was set at 90° with respect to the specimen surface. All binding energies were calibrated to the C 1s graphitic peak position at 284.5 eV. The surface areas of the membranes were measured by means of the Brunauer–Emmett–Teller (BET) method using nitrogen gas (ASAP2020, Micromeritics). The density of carbon fibers was determined by a pycnometer under argon gas.

The electrical conductivities of the carbon papers were measured by the impedance method (Solartron 1260 impedance analyzer) with a 40 mV amplitude signal over the frequency range from 0.1 Hz to 10 MHz at 25°C and 25% RH. The cross-sectional area, A, of the carbon paper was calculated by multiplying the measured width by the measured thickness of the sample. The electrical conductivity σ was calculated using $\sigma = L/AR$, where R is the electrical resistance and L is the distance between the

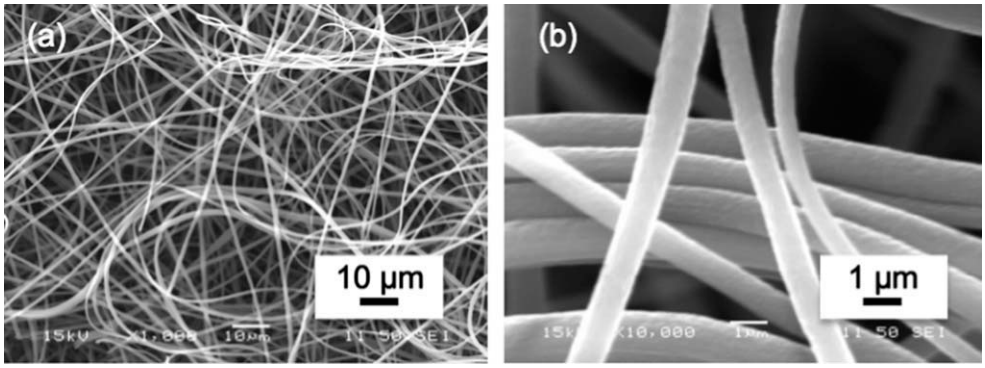

Figure 1 SEM images of electrospun PAN fibers (a) at low magnification (scale bar = 10 μm), (b) at high magnification (scale bar = 1 μm).

electrodes. The wettability of the electrode surface was evaluated by contact angle measurements using a VCA2000 (AST Products, Inc., Billerica, MA). The contact angles were determined by fitting the profiles of at least five 8–10 μL droplets. An AccuPyc 1330 pycnometer was used to measure the densities of electrospun precursors and ECP by using the helium gas displacement technique for measurement.

Electrochemical measurements

Cyclic voltammetry measurements were performed in a standard three-electrode cell with a platinum wire used as the counter electrode and a silver wire used as the pseudo-reference electrode. All potentials were reported versus the silver pseudo-reference electrode. The working electrode was the PAN-based ECP. Copper tape was used to connect the PAN-based carbon electrode with the copper wire. All measurements were made using an Auto-Lab PGSTAT 30 potentiostat, operated with GPES software, version 4.9 (Eco Chemie, Utrech, The Netherlands).

DMF containing 0.1*M* tetrabutylammonium hexafluorophosphate (TBAPF6) was used as the electrolyte solution. Electrochemical measurements were conducted in a glass cell, thermostated at (25 ± 1)°C. Following deoxygenation of 3.9 mL of the DMF/TBAPF6 solution under dry nitrogen with gentle stirring for 30 min, the capacity of the electrode was studied by ramping the potential of the working electrodes from 0 to 1.5 V versus the pseudo-reference electrode, with a scan rate of 0.1 V/s. One hundred microliters of 250 m*M* ferrocene in DMF was then added to the electrolyte solution to test the electrochemical reaction of ferrocene molecules using the developed electrodes. The potential of the working electrodes was ramped several times between 0 and 1.5 V versus the pseudo-reference electrode, with scan rates ranging from 0.005 to 0.1 V/s.

RESULTS AND DISCUSSION

Morphology of PAN electrospun fibers

The morphology of electrospun PAN fibers before hot-pressing is shown in Figure 1, from which it is evident that the fiber surfaces were smooth, and their diameters were 960 ± 250 nm. The PAN fabrics were fluffy, as shown in Figure 1(a). With such a structure, the brittle fracture strength of the fabric, which is related to both the number of contacts between fibers and the bonding force between pairs of fibers, was very weak. All of the hot-press experiments were based on this membrane. The material density of the PAN fibers was about 1.12 g/cm^3.

After hot-pressing for 5, 25, 40, and 60 min and preoxidation, the fiber diameters decreased to 380 ± 130 nm, as shown in Figure 2(a,b). The material density was about 1.21–1.23 g/cm^3 after hot-pressing. No obvious trend was found between the hot-press time and material density of the fibers. The morphology of the fibers was retained without significant changes. Based on thermal gravimetric analysis (TGA) and differential scanning calorimetry (DSC) measurements of PAN fibers, decomposition generally occurs around 290°C, before melting takes place. However, under a 1 metric ton pressure, we speculate that some surface bonding of PAN fibers could occur at lower temperatures and longer heating times. Recent molecular simulations indicate that there exists a mobile surface layer on polymer nanofibers that leads to the joining of fibers at modest temperature (and pressure).[20] Based on a qualitative assessment of the SEM images shown in Figure 2(e), the morphology of the contacts between fibers was changed. It can be seen that the fibers appear to be more extensively fused together after hot-press treatments, with more bonding points formed after hot-pressing at this temperature and pressure, as shown in Figure 2(a,b).

Pretreatment of the electrospun PAN fibers

The acrylonitrile moieties in electrospun nanofibers react with oxygen and undergo chemical changes

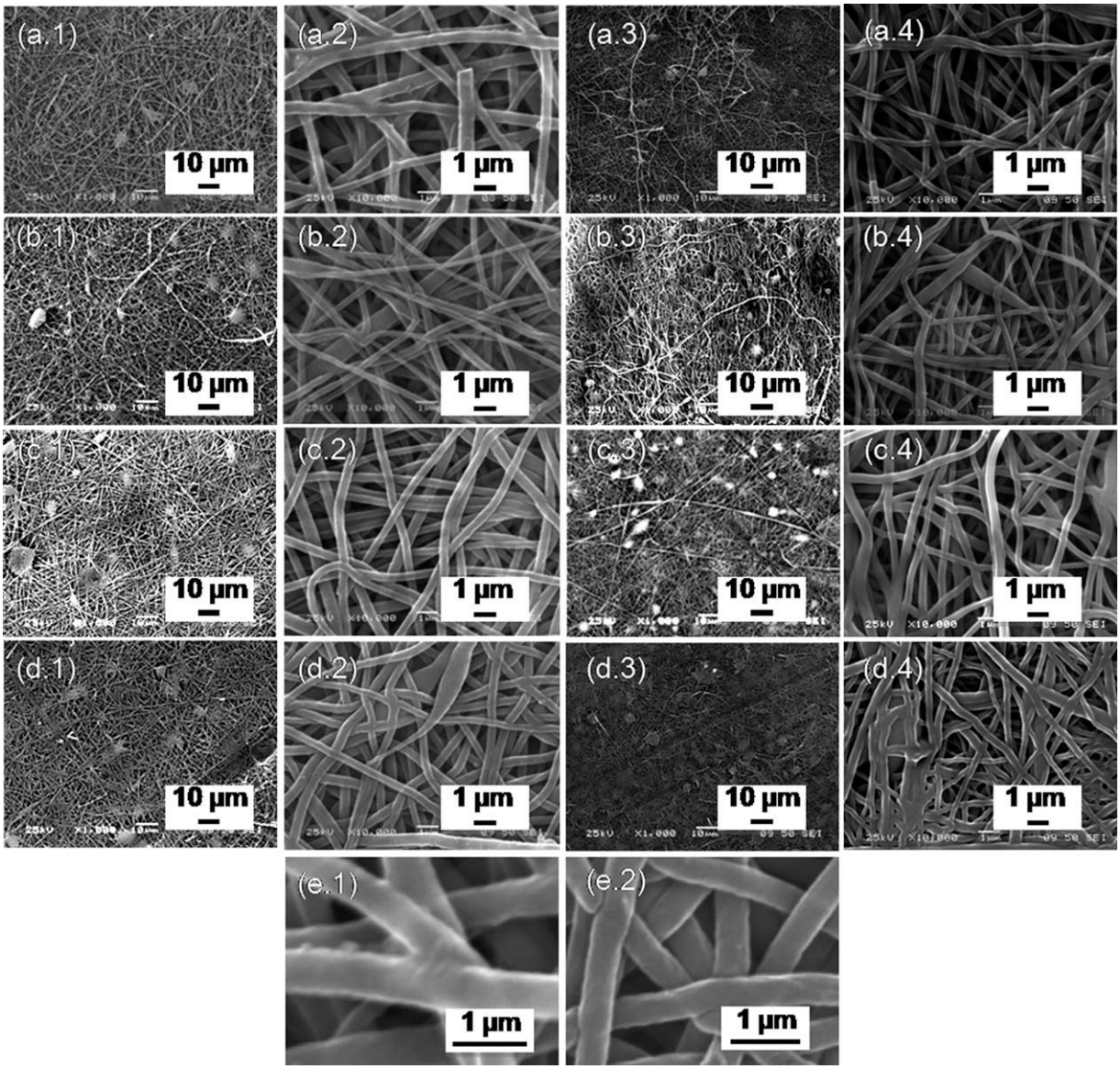

Figure 2 SEM images of electrospun fibers with different hot-press time: (a) 5 min; (b) 25 min; (c) 40 min; (d) 60 min. (.1) PAN fibers after hot-press treatment (scale bar = 10 μm); (.2) larger magnification for PAN fibers after hot-press treatment (scale bar = 1 μm); (.3) PAN-based carbon fibers after carbonization (scale bar = 10 μm); (.4) larger magnification PAN-based carbon fibers after carbonization (scale bar = 1 μm); (e.1) higher magnification PAN fibers after 5 min hot-press treatment (scale bar = 1 μm); (e.2) higher magnification PAN fibers after 45 min hot-press treatment (scale bar = 1 μm).

during the pre-oxidation process in air, forming a "ladder" structure due to cyclization of the nitrile groups in the acrylonitrile moieties.[21] This cyclization reaction raises the melting point and allows the fiber morphology to be retained in the subsequent carbonization.[22] Typically, during pre-oxidation, the PAN-based precursor fiber undergoes a change in color from white to dark brown. The mechanism for coloration is not yet fully understood.

Figure 3 (a) shows XRD patterns from the as-spun electrospun fibers. The two broad diffraction peaks at 17° and ~ 28° are commonly observed in the fiber diffraction patterns of PAN with hexagonal packing.[23,24] After the hot-press treatment and pre-oxidation, a strong diffraction peak appeared at 17° and a weak diffraction peak appeared at 29.5°, corresponding to the (010) and (300) crystallographic reflections, respectively, of the orthorhombic PAN unit cell. When the fibers are hot-pressed for a longer time, the intensities of these two peaks continue to weaken, suggesting a decrease in crystallinity and crystallite size as the linear molecular chains change into the aromatic, ladder structure. Based on the results above, it can be seen that structure of the fibers was changed completely during the process, which is further confirmed by the

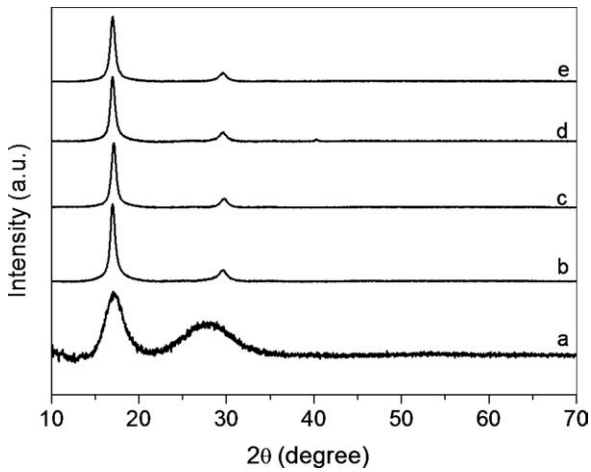

Figure 3 XRD patterns of the electrospun fibers: (a) as-spun electrospun PAN fibers; (b) electrospun PAN fibers after 5 min hot-press; (c) electrospun PAN fibers after 25 min hot-press; (d) electrospun PAN fibers after 40 min hot-press; and (e) electrospun PAN fibers after 60 min hot-press.

FTIR analysis (see Supporting Information Fig. S2 for details).

PAN-based carbon fibers

Morphology of the carbon fibers

During carbonization, a variety of gases (e.g., H_2O, N_2, HCN, and others) were evolved and the carbon content increased to 85 wt % or higher; the process therefore led to the reduction of fiber diameter and the formation of three-dimensional carbonaceous structures. The average diameters of the PAN nanofibers carbonized at 1000°C were reduced to about 280 ± 55 nm in all cases. No evidence of melting during the carbonization step was observed, as shown in Figure 2(c,d).

Compared to the commercial carbon paper (CCP) shown in Figure 4, the inter-fibrillar distances in the plane of the PAN-based ECP was about 1–5 μm while the corresponding distance in the CCP was 10–60 μm. The distance between fibers of the ECP was thus about an order of magnitude smaller than that of the CCP. The densities of the CCP and ECP were 0.44 g/cm^3 and 0.5–0.6 g/cm^3, respectively. The material density of the carbon fiber in the CCP was about 2.1 g/cm^3, which also confirms that the material itself was graphitic. The material density of the ECP was about 1.7–1.8 g/cm^3, which indicates that the material itself contained a higher fraction of amorphous carbon.

Crystallinity

The XRD curves in Figure 5(a–d) were acquired from the carbonized PAN nanofibers after the final carbonization at 1000°C. The PAN-based carbon fibers showed a very broad diffraction peak around 24°, which is attributed to the (002) crystallographic

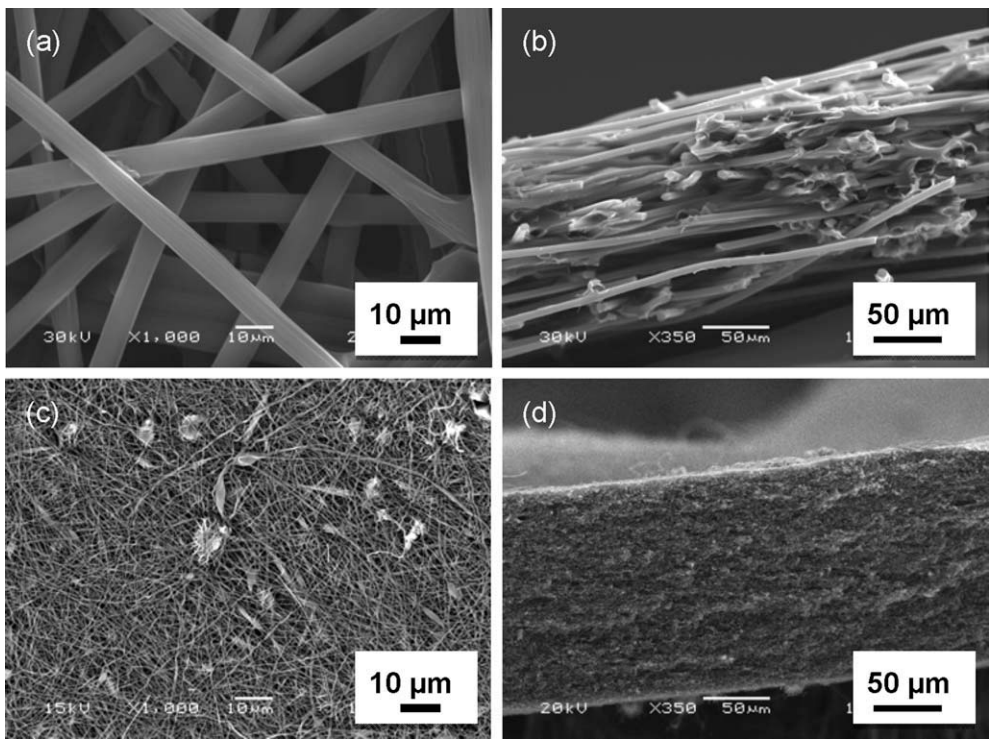

Figure 4 SEM images of carbon papers: (a) CCP; (b) cross-section of CCP; (c) PAN-based ECP (5 min hot press time); (d) cross-section of PAN based ECP.

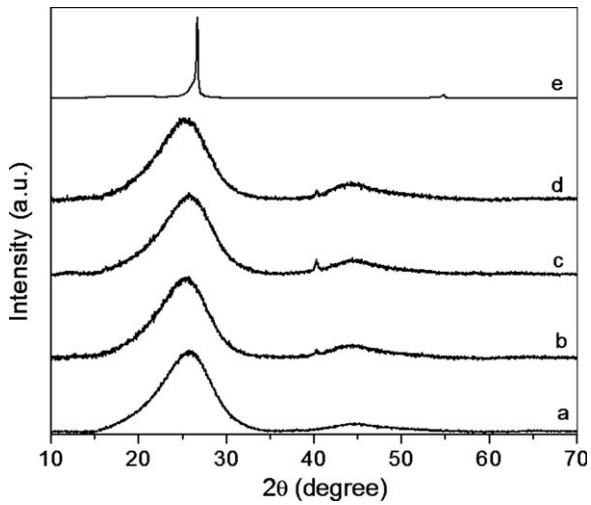

Figure 5 XRD patterns of the PAN-based ECPs with different hot-press time: (a) 5 min; (b) 25 min; (c) 40 min; (d) 60 min; and (e) CCP.

plane of graphite crystallites. This peak shifted slightly towards lower 2θ but exhibited little change in width for materials prepared with increasing hot-press time. Compared to the sharp diffraction peak exhibited by the CCP, the (002) peaks in the ECPs were shifted significantly towards lower 2θ and were much broader. The peak at 43° is characteristic of the (10) reflection in the 2-dimensional lattice of turbostratic carbon. It can be seen that the peak grew with increasing hot-press time. These observations indicate there was very little graphitic structure developed during carbonization at 1000°C. This was to be expected, since PAN-based carbon fibers are generally turbostratic in structure, and such structures are not as ordered as graphite.

Raman spectroscopy

Raman spectroscopy is used widely as a structural probe of carbonaceous materials to analyze the top approximately 50 nm of the film or paper. The Raman spectra of carbonaceous materials show two characteristic features, around 1580 cm^{-1} and 1350 cm^{-1}, called the G and D bands, respectively. The G band is the only feature observed for highly ordered graphite, while the D band is observed when defects and edges are present in the graphitic domains.[25] The I_D/I_G area ratio[25] is often referred to as the "intensity ratio." The Raman spectra for our PAN-based ECP and the results of the Raman analysis can be found in Figure 6. Qualitatively, the relative number of defects in the graphitic domains can be estimated by the I_D/I_G ratio, which increases with increasing hot-press time as shown in Figure 6(b) for spectra acquired with 633 nm excitation lines. Thus, the concentration of defects is shown to increase with longer hot-press treatment.[25] The G band and D band FWHM remained more or less constant.

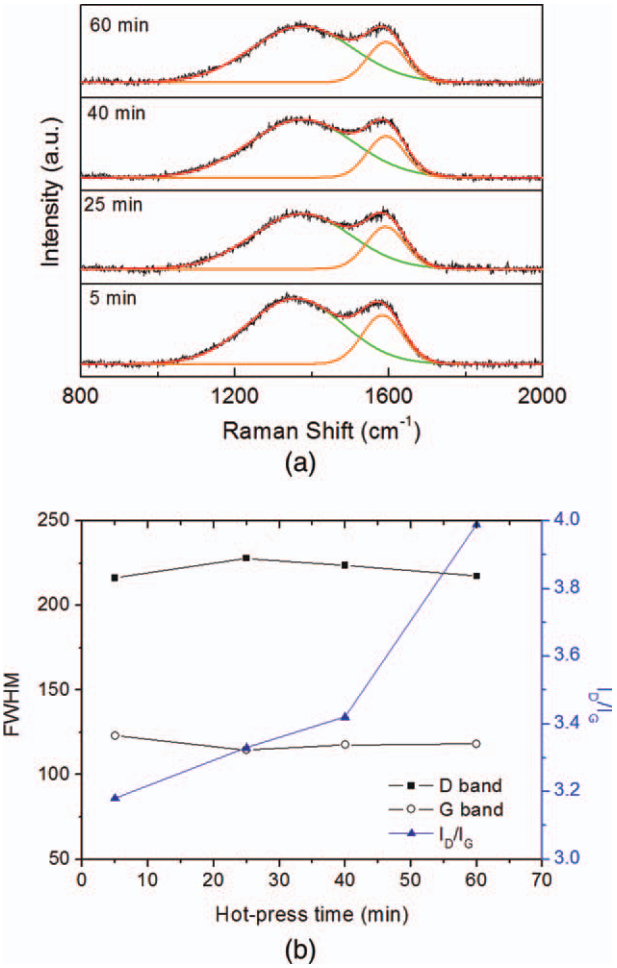

Figure 6 (a) Raman spectra of PAN-based carbon fibers after different hot-press times; (b) the relationship between full width at half maximum (FWHM) and hot-press time. [Color figure can be viewed in the online issue, which is available at wileyonlinelibrary. com.]

XPS

XPS analyzes approximately the top 4 nm of the paper. Table I shows the mass composition of the ECPs in terms of their carbon, oxygen, and nitrogen contents after different hot-press times. The carbon

TABLE I
Elemental Composition of the Carbon Paper Surface (Atom %)

Hot press time	C	O	N
5 min	86.39	3.92	9.69
25 min	88.05	5.31	6.64
40 min	87.00	4.93	8.07
60 min	89.50	4.62	5.89

TABLE II
Deconvolution of the High-Resolution XPS C 1s and N 1s Spectra

Hot-press time (min)	C			N		
	284.4 eV	285.6 eV	288.9eV	398.4 eV	400.5 eV	404 eV
5	0.48	0.41	0.11	0.50	0.41	0.09
25	0.48	0.41	0.11	0.35	0.52	0.13
40	0.47	0.41	0.12	0.41	0.48	0.11
60	0.57	0.36	0.07	0.36	0.46	0.07

content is 86–90%, the oxygen content is 3–6%, and the nitrogen content is unusually high, at 5–10%. It should be mentioned that porous carbon enriched in nitrogen exhibits superior capacitance behavior.[26]

Deconvolution of the high-resolution XPS C 1s spectra yielded several peaks with different binding energies (see Supporting Information in Fig. S4 for details). The carbon 1s lines were decomposed into three components; peaks at 284.7 ± 0.2 and 285.6 ± 0.2 eV were attributed to sp2 and sp3 bonds, respectively, and one at 289 eV was due either to an sp^2 plasmon or a C—O bond. Because oxygen was found in the carbon paper, as seen by XPS, this third line was attributed mainly to the C—O bond.[27] Here, only the relative content of sp^2 and sp^3 is taken into account. As seen in Table II, the sp^2 and sp^3 concentrations on the fiber surface are similar up to a 40 min hot-press time. Deconvolution of the N 1s spectrum yielded three peaks with different binding energies, which can be attributed to pyridine (398.4 eV), aromatic amines, and $-NH_2$ aniline and/or imines C=NH (400.5 eV).[28] A slightly larger peak area around 400.5 eV was observed with longer hot-press times. The O 1s spectrum showed a single peak at 532.1–532.3 eV, which corresponds to C—OH and/or C—O—C groups.[29,30] Although the redox reaction of ferrocene and ferrocenium (c.f., section entitled "Electrochemical properties of ECP electrode") is relatively insensitive to this surface chemistry, other reactions are more strongly dependent.

Surface area and conductivity

Both the specific surface area and the electrical conductivity of carbon paper are important for electrode applications. The surface area of the PAN-based carbon fiber mats decreased with increasing hot-press time, as shown in Figure 7. The BET measurement shows that the surface area of the mat without hot-press treatment was about 7.6 m^2/g, but declined to 1 m^2/g after 1 h of hot-pressing. This is still about three times higher than the surface area of the commercial carbon fiber (0.3 m^2/g) but much less than those of other ECPs without hot-pressing as reported in the literature.[2,26–28] This could be improved by activation in future work.

While the specific surface areas of the hot-pressed ECPs were relatively low compared to those of other ECPs, the electrical conductivities were significantly greater for ECPs processed for longer hot-press times, as shown in Figure 7. The maximum conductivity of ECP was about one half of the conductivity of CCP (80 S/cm). This suggests that the papers prepared with longer hot-press treatment had many more electrically conductive contacts between fibers, since the conductivity of the carbon paper depends not only on the conductivity of the individual nanofibers but also on the contacts between the nanofibers.

Electrochemical properties of ECP electrode

To elucidate the electrochemical properties of these ECP electrodes, cyclic voltammograms of ferrocene molecules were gathered at a series of scan rates ranging from 0.005 V/s to 0.1 V/s, as shown in Figure 8 (a). Ferrocene was used here to elucidate the electrochemical rate constants of the developed electrodes, as this molecule is known to establish electrochemical equilibrium rapidly in non-aqueous electrolyte solutions. Both ferrocene and ferrocenium cations, the product of oxidation of ferrocene, are chemically stable.

The ferrocenyl voltammograms using the ECPs as electrodes provide information on the effects of the morphological and chemical structures of these

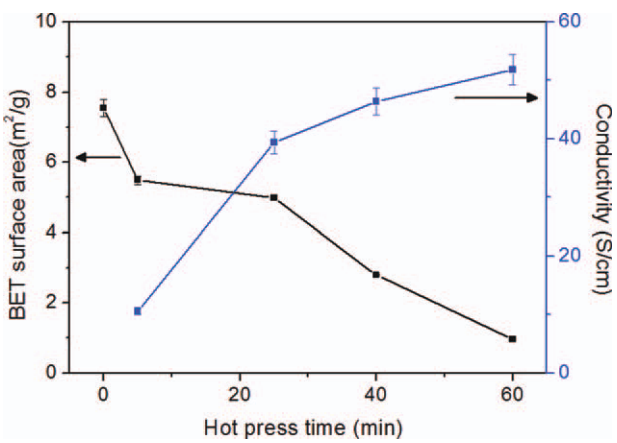

Figure 7 BET surface area and the conductivity of the PAN-based ECP after different hot-press times. [Color figure can be viewed in the online issue, which is available at wileyonlinelibrary.com.]

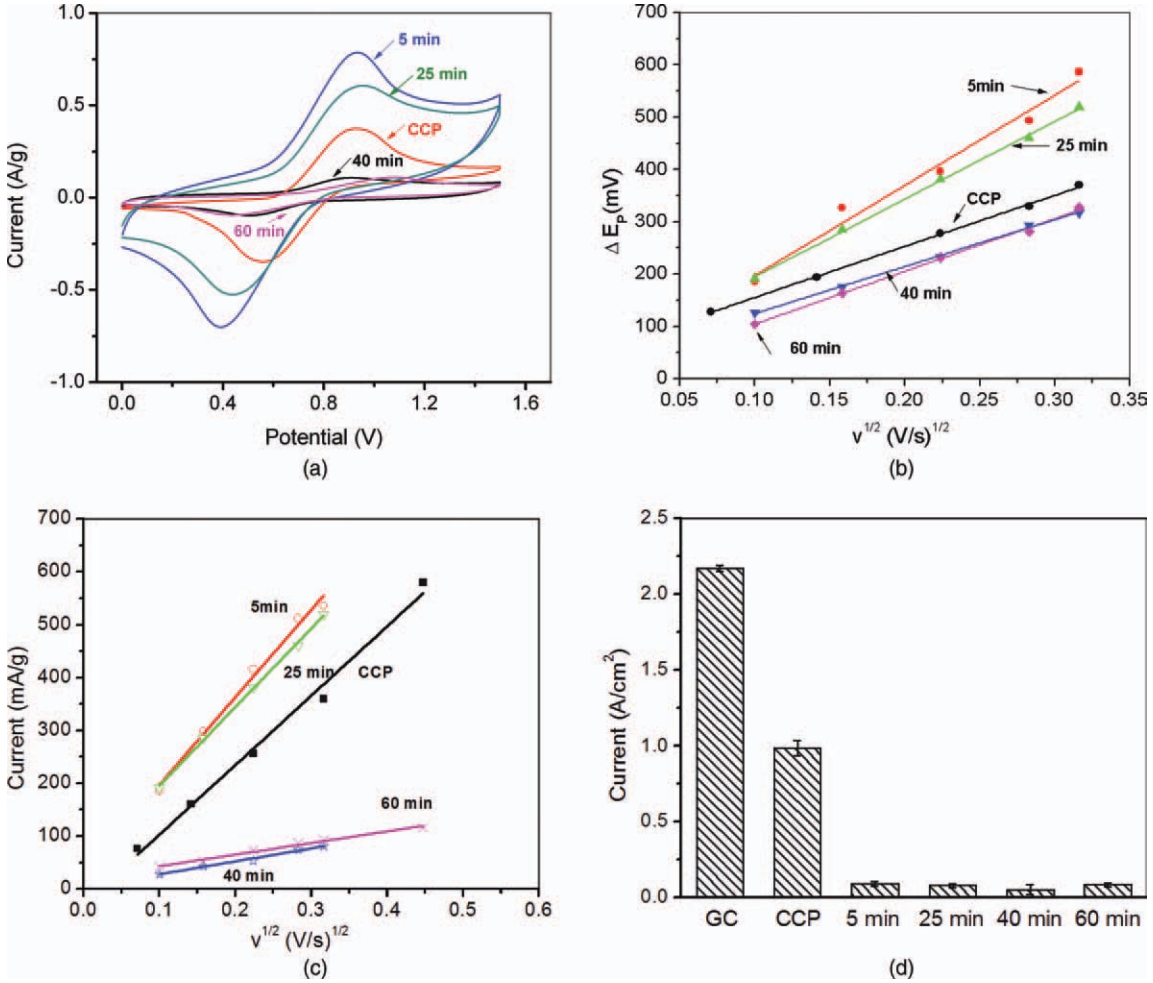

Figure 8 (a) Cyclic voltammograms using 100 μL of 250 m*M* ferrocene in DMF containing 3.8 mL 0.1*M* TBAPF6 at scan rate 0.1 V/s. (b) Linear relationship of the peak potential separation to the square root of scan rate. (c) Linear relationship of peak current to the square root of scan rate. (d) Peak current normalized by surface area for different carbon materials. [Color figure can be viewed in the online issue, which is available at wileyonlinelibrary.com.]

electrodes on the heterogeneous electrochemical reactions. For "fast" electrode kinetics, known as reversible voltammetry, the location of the peak maximum in current in the voltammogram is independent of scan rate. For any reversible one-electron electrochemical reaction, the theoretical potential separation of cathodic and anodic peaks, ΔE_p ($= E_{pc} - E_{pa}$), should be 59 mV at 25°C regardless of scan rate.[30] Figure 8(a) shows a series of voltammograms recorded at different scan rates for the ECPs, while Figure 8(b) shows that ΔE_p increased progressively with the square root of the scan rate, attributed to "slow" electrode kinetics, in which an electrochemical "Nernst" equilibrium is not established on the electrode surface at the scan rates used. It was found that ΔE_p decreased with increasing hot-press time.

The standard rate constant at the standard potential,[31] k^0, reflects the electron transfer property according to the value of ψ, which can be determined from the peak potential separation ΔE_p as reported in Table I of Nicholson.[32] According to the Nicholson model,[32]

$$\psi = \gamma^{\alpha} k^0 (\pi a D_0)^{-1/2} \tag{1}$$

and

$$a = \frac{nFv}{RT} \tag{2}$$

The parameters are $\gamma = (D_0/D_R)^{1/2}$, where D_0 and D_R are the diffusion coefficients of oxidized and reduced species, respectively (in our case, $D_0 = D_R = 1.1 \times 10^{-5}$ cm^2/s), v is the scan rate, n is the stoichiometric number of electrons consumed in the electrode reaction (one, in this case), and F is the Faraday constant.

In this way, we obtain a series of values on the order of magnitude 10^{-3} to 10^{-4} cm/s for k^0 for the ECP electrode at the lowest scan rate (0.01 V/s), which is of the order of magnitude typical of semiconductors and especially of carbon materials.

Peak currents depend on the analyte concentration and the stability of the electro-generated species. Figure 8(c) shows that the peak currents generated per mass of electrode were proportional to the square root of the scan rate, suggesting that the electron processes were diffusion-controlled. The anodic to cathodic current ratio was unity for all scan rates, indicating that the ferrocene electrochemical reaction for both ECP and CCP was quasi-reversible. The peak current for a quasi-reversible system is given by

$$i_p = (2.69 \times 10^5) n^{1.5} A D^{0.5} v^{0.5} C_0^* K(\Lambda, \alpha) \quad (3)$$

with

$$\Lambda = \frac{k^0}{(\alpha D)^{1/2}} \quad (4)$$

where A is the effective surface area of the electrode, C_0* is the bulk concentration of the ferrocene/ferrocenium species, D is the diffusion coefficient of the ferrocene/ferrocenium species in solution, K is a function of the parameters Λ and the electron transfer coefficient $\alpha = 0.5$.

From eq. (3), it can be seen that the peak current, i_p, should be directly proportional to the effective surface area, the square root of the diffusion coefficient and the scan rate if K is constant. The peak currents measured for ECP electrodes with hot-press treatments of 5 min and 25 min are approximately 1.5 times larger than those for the CCP electrode.

For the ECP, the shorter hot-press treatment gives rise to a less reversible electrochemical reaction (larger ΔE_p), whose behavior can be correlated with the morphology of electrode. Longer hot-press treatment of ECP produces a denser electrode with lower surface area, as shown in Figure 8, which reduces the area of contact between the redox species and the electrode, and at the same time increases the reversibility (smaller ΔE_p) of the electrochemical reaction. The larger contact area obtained with shorter hot press treatment (as evidenced by the high current response), on the other hand, gives rise to a more irreversible electrochemical reaction, possibly due to the more porous structure of the materials obtained with short hot-press times.

As mentioned above, for slow electron transfer kinetics, the current is related to the effective surface area of the electrode and/or effective diffusivity of the redox-active species. In order to show the effect of the surface area of the electrode, the voltammograms reported in Figure 8(c) have been normalized by this surface area, assuming that the BET-determined value is a good measure of the effective surface area in all cases. Figure 8(d) shows the normalized currents for glassy carbon (GC) (2.2 A/m^2), CCP ($\sim$ 1 A/m^2), and all thePAN-based ECPs ($\sim$ 0.08 A/m^2). Based on the analysis above, it can be concluded that the main contribution to the large current mass density is the larger surface area of the ECP electrode. The current surface density could be improved after graphitization. This will be reported in our future work.

CONCLUSION

PAN-based ECPs have been fabricated and characterized for microstructure, specific surface area, electronic conductivity, and utility as electrodes for electrochemical redox reactions. A hot-press treatment was performed to modify the electrospun PAN membrane before it was stabilized and carbonized. The electrospun PAN fibers could melt at modest temperature and pressure, resulting in bonding between fibers at around 200°C. With increasing hot-press time, the surface area of the membrane decreased. The resulting PAN-based carbon paper has potential application as an electrode in many electrochemical processes. It was found that the carbon nanofibers became less graphitic and less ordered with increasing hot press time, while the electrical conductivities increased. These results show that a higher surface area electrode produced with a short hot-press time can provide a reasonable electron transfer rate for electrochemical reaction. Electrodes with better conductivity were produced using longer hot-press times, which can provide smaller peak potential separation. It is expected that further graphitization in the system should improve the electrode performance for electrochemical analysis.

References

1. Mathur, R. B.; Maheshwari, P. H.; Dhami, T. L.; Sharma, R. K.; Sharma, C. P. J Power Sources 2006, 161, 790.
2. Kim, C.; Choi, Y. O.; Lee, W. J.; Yang, K. S. Electrochim Acta 2004, 50, 883.
3. Cantwell, W. J.; Morton, J. Composites 1991, 22, 347.
4. Lyons, J.; Ko, F. Polym New 2005, 30, 1.
5. Li, D.; Xia, Y. Adv Mater 2004, 16, 1151.
6. Rutledge, G. C.; Fridrikh, S. V. Adv Drug Deliv Rev 2007, 59, 1384.
7. Bhattacharjee, P. K.; Rutledge, G. C. Electrospinning and Polymer Nanofibers: Process Fundamentals, in Comprehensive Biomaterials, P. Ducheyne, Ed., Ch 39, Elsevier: Oxford (in press).
8. Moon, S.; Farris, R. J. Carbon 2009, 47, 2829.
9. Zhou, Z. P.; Lai, C. L. Zhang, L. F.; Qian, Y.; Hou, H. Q.; Reneker, D. H.; Fong, H. Polymer 2009, 50, 2999.
10. Zussman, E.; Chen, X.; Ding, W.; Calabri, L.; Dikin, D. A.; Quintana, J. P.; Ruoff, RS. Carbon 2005, 43, 2175.
11. Bui, N. N.; Kim, B. H.; Yang, K. S. Carbon 2009, 47, 2538.
12. Hiralal, P.; Imaizumi, S.; Unalan, H. E.; Matsumoto, H.; Minagawa, M.; Rouvala, M.; Tanioka, A.; Amaratunga, G. A. J. ACS Nano 2010, 4, 2730.

13. Imaizumi, S.; Matsumoto, H.; Suzuki, K.; Minagawa, M.; Kimura, M.; Tanioka, A. Polym J 2010, 41, 1124.
14. Zhang, Z. Y.; Li, X. H.; Wang, C. H.; Fu, S. W.; Liu, Y. C.; Shao, C. L. Macromol Mater Eng 2009, 294, 673.
15. Ju, Y. W.; Park, S. H.; Jung, H. R.; Lee, W. J. Electrochem Soc 2009, 156, A489.
16. Kim, C.; Jeong, Y.; Ngoc, BTN. Yang, K. S.; Lee, JW; Kojima, M; Kim, YA; Endo, M. Small 2007, 3, 91.
17. Na, H. N.; Zhao, Y. P.; Zhao, C. G.; Zhao, C.; Yuan, X. Y. Polym Eng Sci 2008, 48, 934.
18. Na, H. N.; Li, Q. Y.; Sun, H.; Zhao, C.; Yuan, X. Y. Polym Eng Sci 2009, 49, 1291.
19. Shin, Y. M.; Hohman, M. M.; Brenner, M. P.; Rutledge, G. C. Polymer 2001, 42, 9955.
20. Buell, S.; Rutledge, G. C.; Van Vliet, K. J. ACS Appl Mater Interfaces 2010, 2, 1164.
21. Rahaman, M. S. A.; Ismail, A. F.; Mustafa, A. Polym Degrad Stab 2007, 92, 1421.
22. Fitzer, E. Carbon 1989, 27, 621.
23. Boguslavsky, L.; Margel, S. Glass Phys Chem 2005, 31, 102.
24. Hou, X. X.; Yang, X. P.; Zhang, L. Q.; Waclawik, E.; Wu, S. Z. Mater Des 2010, 31, 1726.
25. Pimenta, M. A.; Dresselhaus, G.; Dresselhaus, M. S.; Cancado, L. G.; Jorio, A.; Saito, R. Phys Chem Chem Phys 2007, 9, 1276.
26. Lota, G.; Grzyb, B.; Machnikowska, H.; Machnikowski, J.; Frackowiak, E. Chem Phys Lett 2005, 404, 53.
27. Ermolieff, A.; Chabli, A.; Pierre, F.; Rolland, G.; Rouchon, D.; Vannuffel, C.; Vergnaud, C.; Bavlet, J.; Semeria, M. N. Surf Interface Anal 2001, 31, 185.
28. Mangun, C. L.; Benak, K. R.; Economy, J.; Foster, K. L. Carbon 2001, 39, 1809.
29. Yue, Z. R.; Jiang, W.; Wang, L.; Gardner, S. D.; Pittman, C. U. Carbon 1999, 37, 1785.
30. Swiatkowski, A.; Pakula, M.; Biniak, S.; Walczyk, M. Carbon 2004, 42, 3057.
31. Bard, A. J.; Faulkner, L. R. Electrochemical Methods: Fundamentals and Applications, 2nd ed.; Wiley: New York, 2000; p 237.
32. Nicholson, R. S. Anal Chem 1965, 37, 1351.